BIOCHEMISTRY
including biophysical chemistry & molecular biology

Article

pubs.acs.org/biochemistry

Kinetics and Fidelity of Polymerization by DNA Polymerase III from *Sulfolobus solfataricus*

Robert J. Bauer, Michael T. Begley, and Michael A. Trakselis*

Department of Chemistry, University of Pittsburgh, Pittsburgh, Pennsylvania 15260, United States

Supporting Information

ABSTRACT: We have biochemically and kinetically characterized the polymerase and exonuclease activities of the third B-family polymerase (Dpo3) from the hyperthermophilic Crenarchaeon, *Sulfolobus solfataricus* (*Sso*). We have established through mutagenesis that despite incomplete sequence conservation, the polymerase and exonuclease active sites are functionally conserved in Dpo3. Using pre-steady-state kinetics, we can measure the fidelity of nucleotide incorporation by Dpo3 from the polymerase active site alone to be 10^3–10^4 at 37 °C. The functional exonuclease proofreading active site will increase fidelity by at least 10^2, making Dpo3 comparable to other DNA polymerases in this family. Additionally, Dpo3's exonuclease activity is modulated by temperature, where a loss of promiscuous degradation activity can be attributed to a reorganization of the exonuclease domain when it is bound to primer–template DNA at high temperatures. Unexpectedly, the DNA binding affinity is weak compared with those of other DNA polymerases of this family. A comparison of the fidelity, polymerization kinetics, and associated functional exonuclease domain with those previously reported for other *Sso* polymerases (Dpo1 and Dpo4) illustrates that Dpo3 is a potential player in the proper maintenance of the archaeal genome.

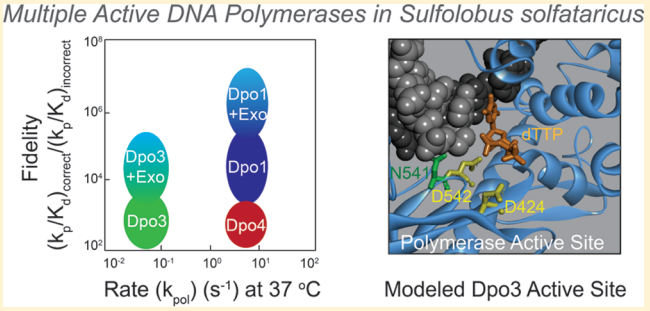

Over the past 20 years, many additional DNA polymerases have been discovered within the genome of most organisms. This raises the question of how multiple DNA polymerases are regulated with regard to their individual functions for the maintenance of the organism's genetic material. DNA polymerases have been divided into six main families (A, B, C, D, X, and Y).[1,2] It is clear that B-family DNA polymerases provide the bulk of DNA synthesis during replication and that X- and Y-family DNA polymerases act only under special circumstances in various DNA repair pathways.[3] In addition to the 12 other DNA polymerases in humans, there are three B-family DNA polymerases that act in both the initiation and the elongation phases of DNA replication.[4]

DNA polymerases from the B-family are generally robust and accurate enzymes with inherent nucleotide specificities augmented further by exonuclease proofreading domains that give nucleotide fidelities of $>10^8$, or one error every 10^8 bases incorporated.[5] They become processive for >10000 bases after complexation with their respective processivity factors or clamps.[6] The leading (ε) and lagging (δ) strand polymerases[7] as well as the pol-α primase complex[8] are the three B-family polymerases found in humans. There are few significant mechanistic differences in enzymatic activities between ε and δ, except for their strand specificities that are not fully understood.[9] Pol-α primase, on the other hand, is able to synthesize short oligoribonucleotide primers that can be extended further through incorporation of deoxyribonucleotides on both strands to initiate replication elongation.[10,11]

The DNA processing enzymes in archaea have been shown to be more similar to those of eukaryotes than bacteria and serve as a simplified model for understanding more complex eukaryotic activities.[12−15] Of the two main phyla in archaea, Euryarchaea have both B-family and D-family (unique to this archaeal phyla) DNA polymerases,[16] whereas Crenarchaea have B-family and Y-family DNA polymerases.[17,18] Crenarchaea have a more conserved arsenal of eukaryotic-like DNA polymerases; however, the metal binding domain of eukaryotic polymerases (ε and δ) may have evolved from the Euryarchaeal D-family polymerases instead.[19] The Crenarchaeon *Sulfolobus solfataricus* (*Sso*) has within its genome three B-family polymerases (Dpo1, Dpo2, and Dpo3), similar in number to the main analogous DNA polymerases (α, δ, and ε) found in humans. Both the proposed DNA replication polymerase, Dpo1, and the lesion bypass polymerase, Dpo4, have been well characterized with regard to their nucleotide incorporation mechanisms,[20,21] fidelities,[22,23] and structures.[24,25] Dpo2 and Dpo3 have been identified by sequence homologies,[26,27] and until very recently, their activities had not been biochemically characterized.[28]

Here, we have characterized the mechanism and kinetics of polymerization, exonuclease proofreading, and DNA binding activities of the third B-family DNA polymerase from *S. solfataricus*, Dpo3. We have identified and mutated conserved

Received: December 7, 2011
Revised: January 23, 2012
Published: February 17, 2012

amino acids in both the polymerization and exonuclease domains to confirm conservation and quantify their respective activities. Surprisingly and unlike other DNA polymerases, Dpo3 binds weakly to DNA requiring higher concentrations of enzyme for efficient nucleotide incorporation. This weak binding can be attributed to a mutation in the universally conserved Pol I motif. We have also quantified the selectivity of nucleotide incorporation for all 16 possible combinations into undamaged DNA templates using pre-steady-state kinetics. Circular dichroism analyses suggest that Dpo3 is a stable enzyme with a T_m of >94 °C, although the thermostability of the specific exonuclease domain may be regulated by substrate binding and temperature. The nucleotide incorporation rates, fidelity values, and exonuclease results are compared to those of the more thoroughly characterized *Sso* DNA polymerases (Dpo1 and Dpo4) to gain a better understanding of the diversity of DNA polymerase functions in the cell.

MATERIALS AND METHODS

Materials. Oligonucleotide substrates were purchased from Integrated DNA Technologies (IDT, Coralville, IA) and are listed in Table S1 of the Supporting Information. DNA strands with more than 28 nucleotides were gel-purified utilizing denaturing acrylamide gel electrophoresis.[29] Radioactive [γ-^{32}P]ATP was purchased from MP Biomedicals (Solon, OH). Optikinase (USB, Cleveland, OH) was used for 5′-end labeling of DNA substrates according to manufacturer's protocols. Radiolabeled primers were added to cold complementary template strands at a ratio of 1:1.2 to ensure proper annealing. Annealing was performed by heating the sample to 95 °C for 5 min, followed by slow cooling to room temperature for at least 2 h. Commercial enzymes were from NEB (Ipswich, MA). All other chemicals were analytical grade or better.

Dpo3 Protein Purification. Dpo3 was amplified from *S. solfataricus* P2 genomic DNA (ATCC catalog no. 35092) with Pfx50 polymerase (Invitrogen, Carlsbad, CA). The gene was initially subcloned into pGEM-T (Promega, Madison, WI) and then ligated into pET30a (EMD Chemicals, Gibbstown, NJ) using the *Nde*I and *Xho*I restriction sites included in the primer sequences (Supporting Information) to allow for expression of a C-terminal 6XHis tag. The DNA polymerase (D424A, D542A, and D424A/D542A) and exonuclease (D226A, D228A, D234A, and D236A) mutant constructs were created using a standard QuikChange protocol (Agilent, Santa Clara, CA) with KAPA HiFi DNA polymerase (KAPA Biosystems, Woburn, MA).

BL21(DE3) Rosetta 2 cells containing the various pET30a-Dpo3 constructs were grown at 37 °C, and protein expression was autoinduced as described previously.[30] Cell pellets were resuspended in 50 mM sodium phosphate buffer (pH 7.0), 50 mM NaCl, and 5 mM β-mercaptoethanol. The cells were lysed by the addition of lysozyme and sonicated. After centrifugation, the supernatant was treated with heat at 70 °C for 20 min to precipitate host proteins and centrifuged again. The supernatant containing Dpo3 was purified using a Ni^{2+} column (Thermo Fisher, Waltham, MA) and eluted with a step gradient of 500 mM imidazole. Further purification was performed using an ATKA Prime FPLC system with HiTrap DEAE and heparin columns (GE Healthcare, Piscataway, NJ) and elution with a linear gradient to 1 M NaCl. Separation of a major degradation product can be performed using a pH gradient from 8.5 to 7.9 and a MonoQ column (GE Healthcare). Final cleanup and sizing were performed with a Superdex 200 26/60 column (GE Healthcare). The extinction coefficient for Dpo3 was determined to be 117893 M^{-1} cm^{-1}.[31] Typical yields of purified protein were >3 mg/L of cells.

Polymerase Activity Assays. Standard assays were performed in polymerization buffer [20 mM Tris-acetate (pH 7.5), 100 mM potassium acetate, and 10 mM magnesium acetate] containing 36 nM primer−template DNA (ptDNA) and various concentrations of Dpo3 as indicated. Prior to initiation by addition of dNTPs, the reaction components were incubated for 5 min at the reaction temperature. Experiments were conducted at the temperatures, polymerase concentrations, dNTP concentrations, and times indicated in each figure legend. Reactions were terminated by the addition of an equal volume of a formamide quench (100 mM EDTA, 0.1% SDS, and 79% formamide). To examine the products for short templates, we used denaturing gels [20% acrylamide, 8 M urea, and TBE buffer (45 mM Tris-borate and 1 mM EDTA)]. Phosphor screens were then exposed to the gels for a minimum of 4 h, imaged with a Storm 820 Phosphorimager (GE Healthcare), and quantified using ImageQuant version 5.0.

Divalent Cation Optimization. Optimization of divalent cations was performed under polymerase activity assay reaction conditions as detailed above; however, the concentration of the divalent metal, M^{2+} (Mg^{2+} or Mn^{2+}), was varied. Reactions were quenched and analyzed as described above for standard polymerase reactions. Data obtained from M^{2+} titration reactions were fit to a Michaelis−Menten equation with a cooperativity (n) parameter:

$$[\text{product}] = \frac{V_{max}[M^{2+}]^n}{K_m{}^n + [M^{2+}]^n} \quad (1)$$

where V_{max} is the maximal rate, K_m is the Michaelis constant, and $[M^{2+}]$ is the concentration of the divalent cation included in the reaction. For those reactions where inhibition was observed at higher concentrations of M^{2+}, an inhibition reaction equation was used instead:

$$[\text{product}] = \frac{V_{max}[M^{2+}]}{K_m + [M^{2+}]\left(1 + \frac{[M^{2+}]}{K_i}\right)} \quad (2)$$

where K_i is the inhibition constant.

Polymerase Fidelity. Fidelity assays were performed as detailed above for polymerase reactions; however, each preincubated reaction mixture contained 9.6 nM DNA and 2 μM Dpo3 (D236A), and each reaction was initiated with varying concentrations of dNTPs. Samples were removed and placed in a 1:1 ratio into quench at the time points indicated in each figure legend. The time course of product formation was fit to a single-exponential equation for each concentration of dNTP:

$$[\text{product}] = A(1 - e^{-k_{obs}t}) \quad (3)$$

where A represents the reaction amplitude, k_{obs} is the observed polymerase rate, and t is the time in seconds. The observed rates extracted from the time courses of product formation for each dNTP concentration were then plotted versus their respective dNTP concentrations and fit to a hyperbolic equation:

$$k_{obs} = k_p[\text{dNTP}]/([\text{dNTP}] + K_d) \quad (4)$$

where k_p is the maximal rate of dNTP incorporation and K_d is the dissociation constant for the incoming nucleotide.

dx.doi.org/10.1021/bi201799a | *Biochemistry* 2012, 51, 1996−2007

Fluorescence Anisotropy DNA Binding Assays. Anisotropy assays were performed in polymerization buffer, in the absence of dNTPs with 1 nM ssDNA or ptDNA, where a Cy3 fluorescent label was placed on the 5′-end of the single strand or template strand, respectively, and varying concentrations of Dpo3 (D236A) as depicted. Anisotropy values were obtained using a Fluoromax-3 fluorimeter with automated polarizers (HORIBA Jobin Yvon, Edison, NJ). Cy3 was excited at 550 nm during 1 s integration times, and data points represent averages of five consecutive readings. The reported anisotropy values are the average and standard error from three independent titrations. The absolute fluorescence emission (565 nm) was unchanged during the course of the titration, eliminating the possibility that Dpo3 binds directly to Cy3. The fluorescence anisotropy (r) was calculated using the following equation:

$$r = \frac{I_{VV} - GI_{VH}}{I_{VV} + 2I_{VH}} \quad (5)$$

where I is the polarization intensity and the subscripts V and H denote vertically and horizontally polarized light, respectively. G is a correction factor for any differences in the intensity of horizontally and vertically polarized light and is calculated automatically by FluorEssence version 2.5.2.0.

The change in anisotropy was fit to a single binding equation:

$$r = \frac{A[\text{Dpo3}]}{K_d + [\text{Dpo3}]} \quad (6)$$

where A is the reaction amplitude and K_d is the dissociation constant for the interaction between Dpo3 and DNA.

Exonuclease Assays. Standard exonuclease assays were performed in polymerization reaction buffer containing 18 nM ptDNA and 2 μM Dpo3. Prior to initiation by addition of DNA, the reaction components were incubated for 5 min at 55 °C, unless otherwise indicated. Experiments were performed for the times indicated in each figure legend. Reactions were quenched and analyzed as described for polymerase reactions.

Circular Dichroism (CD) Denaturing Measurements. Circular dichroism (CD) experiments for monitoring conformational changes of either polymerase alone or polymerase bound to DNA were performed using a DSM 17 instrument (Olis Inc., Bogart, GA) using a 1 mm path length cell. The experiments were conducted either in the presence or in the absence of DNA hairpin (2 μM) and Dpo3 (4 μM). The molar ellipticity (Θ) at 222 nm was monitored over a temperature range from 20 to 95 °C in 2 °C intervals controlled by a Peltier temperature controller. The spectra from at least three separate scans were averaged and analyzed as described previously.[32]

Homology Modeling and Alignment. Local and global sequence alignments were performed using ClustalW2 analysis (http://www.ncbi.nlm.nih.gov/blast/bl2seq/wblast2.cgi). The homology model of Dpo3 was created by threading the global alignment of Dpo3 with Dpo1 onto the structure of Dpo1 [Protein Data Bank (PDB) entry 1S5J][25] using SWISS-MODEL.[33] The DNA and incoming nucleotide were modeled into the active site of the homology model of Dpo3 by aligning the polymerase active site of the RB69 gp43−DNA−dTTP ternary complex (PDB entry 1IG9)[34] with the homology model of Dpo3 using PyMol (http://www.pmol.org).

RESULTS

Conditions for Optimal Polymerase Activity of Dpo3. After purification of wild-type (WT) Dpo3 to homogeneity (Figure 1A), we characterized the buffer conditions required for maximal polymerase activity in 100 mM NaCl at 60 °C.

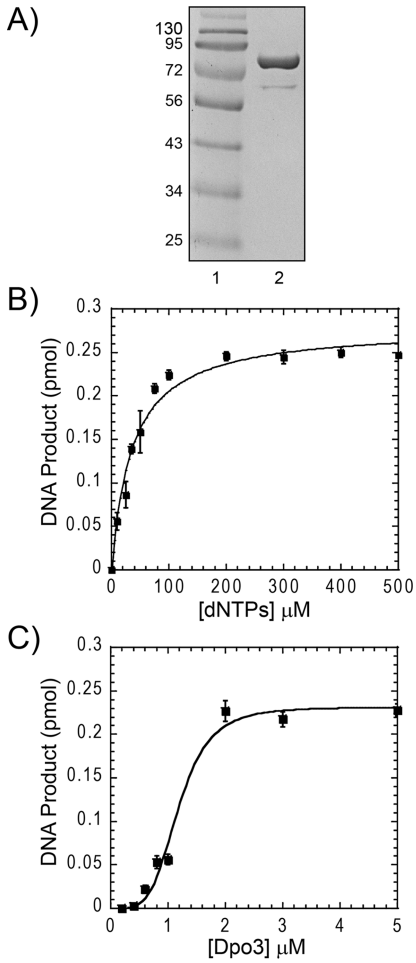

Figure 1. (A) Purified Dpo3 on a Coomassie-stained sodium dodecyl sulfate−polyacrylamide gel electrophoresis gel: lane 1, protein markers; lane 2, Dpo3 (88 kDa). (B) Optimization of dNTP concentrations on total DNA product produced by 2 μM Dpo3 on ptDNA in Tris (pH 7.5) and 10 mM Mg^{2+} at 70 °C. The K_m for dNTPs (36 ± 5 μM) was determined from the average of three independent experiments fit to eq 1. (C) Effect of Dpo3 concentration on the total amount of DNA product produced using a long ptDNA template. Reactions were performed in Tris (pH 7.5), 200 μM dNTPs, and 10 mM Mg^{2+} at 70 °C for 10 min. The apparent dissociation constant (K_d') for Dpo3 activity (1.2 ± 0.1 μM) was determined from the average of three independent experiments fit to eq 1. The cooperativitiy parameter (n) was equal to 4.4 ± 1.1.

Purification with a gel-filtration column for size selection was required for maximal polymerase activity, although no significant shift in molecule size was noted in the chromatogram. Neither HEPES nor Tris buffers nor varying the pH over a limited physiological range (6.0−8.5) produced a significant change in the polymerase activity of Dpo3 (Figure S1A of the Supporting Information). Maximal activity was observed with 20 mM Tris between pH 7 and 8.5, so a pH of 7.5 was used in all subsequent reactions. A comparison of the polymerization ability in our buffer compared with that used previously[28] showed no significant difference in the rate of incorporation (data not shown).

The importance of divalent cations in the nucleotide incorporation process has been well characterized, where the

quantity of product extension is known to be dependent on metal concentration.[35] We performed polymerase reactions while varying the concentration of Mg^{2+} (Figure S1B of the Supporting Information) and fit the data to eq 1 with an observed K_m of 1.43 ± 0.08 mM. Identical experiments with Mn^{2+} showed an inhibition at concentrations of >0.5 mM. On the basis of these results, we chose to include 10 mM Mg^{2+} in the reaction buffer. Similarly, the optimal concentration of dNTPs was monitored (Figure 1B), where the K_d for incoming nucleotides was determined to be 36 ± 5 μM. dNTPs (200 μM) were included in all subsequent polymerase reactions unless indicated otherwise. As a note, the exonuclease activity present in WT Dpo3 reduced the detected amount of fully extended product slightly from the theoretical maximum.

Having established appropriate reaction buffer conditions, we titrated Dpo3 to determine the optimal concentration for maximal activity (Figure 1C). Interestingly, very low activity levels were observed until a reaction concentration of 750 nM was reached. The data required a cooperativity coefficient for an appropriate fit to extract the apparent dissociation constant (K_d') equal to 1.2 ± 0.1 μM. The sigmoidal shape of the curve indicates that the concentration of the polymerase is critical for binding and associated activity. Further kinetic assays were performed at 2 μM Dpo3 determined to provide for maximal activity unless indicated otherwise.

Thermostability of Dpo3. The optimal reaction temperature was determined by examining the total amount of product synthesized from ptDNA at temperatures varying from 37 to 70 °C in a 10 min reaction (Figure 2A). We observed maximal polymerase product formation at 65 °C. Reactions in the absence of dNTPs monitored the exonuclease activity and were maximal at 55 °C, and their rates decreased as the temperature was increased further. The purification protocol included a 70 °C incubation step that typically eliminates any background nuclease activity. The exonuclease activity of any contaminating nucleases from *Escherichia coli* should be maximal around 37 °C and decrease above 45 °C. The parallel increases in both polymerase and exonuclease activities from 37 to 55 °C show that the observed exonuclease activity is intrinsic to the polymerase.

Although the polymerization activity of Dpo3 is maximal above 65 °C, to assay the thermostability of the Dpo3 protein structure, we preincubated the WT polymerase at 70 °C for various times and then initiated the reaction by adding dNTPs or DNA to monitor polymerase or exonuclease activity, respectively (Figure 2B). Extension to the full-length product from the primer–template form was used to evaluate any loss of polymerization activity. Even after incubation at 70 °C for 55 min, the loss of DNA polymerase activity was minimal. The reduction in exonuclease activity was slightly greater, but 55% of the activity remained after the 55 min high-temperature incubation period.

To gain a more direct measure of protein structure thermostability, we used circular dichroism (CD) to monitor the change in molar ellipticity at 222 nm as a function of temperature in the absence and presence of hairpin DNA (Figure 2C). The protein structure of Dpo3 is highly thermostable with an estimated melting temperature (T_m) of >94 °C. The data could not be quantified accurately because the maximum of the denatured curve was not apparent at 100 °C. We also note a small but reproducible unfolding event that occurs at 63 °C. This may be localized unfolding of a small thermally unstable domain within Dpo3. In the presence of ptDNA, the T_m for Dpo3 shifts slightly higher (~96 °C) and the local unfolding event at 63 °C disappears.

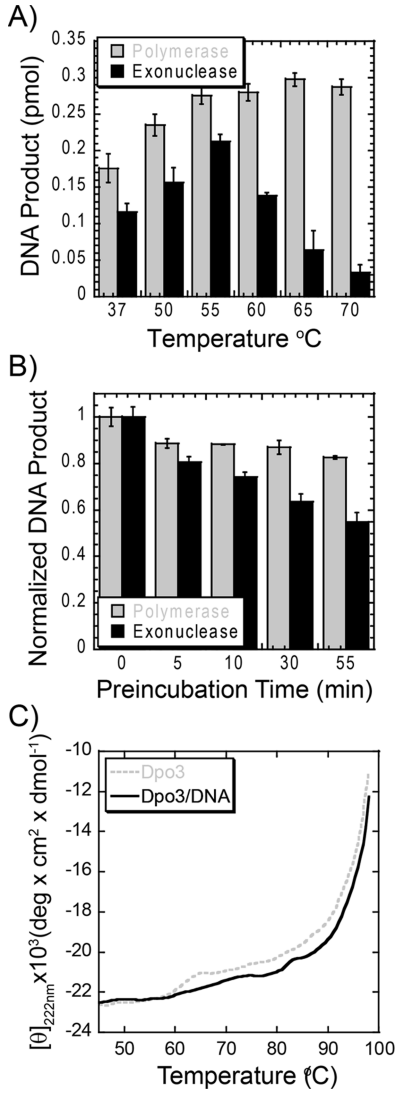

Figure 2. (A) Temperature dependence of 2 μM Dpo3 (WT) in 50 mM Tris (pH 7.5), 10 mM Mg^{2+}, and 200 μM dNTPs on polymerase (gray) and exonuclease (black) activities on ptDNA (36 nM) in a 10 min reaction. The reported values and errors are the average of three independent experiments. (B) Thermostability of 2 μM Dpo3 (WT) after preincubation at 70 °C for the indicated time points. Quantification of product formation for polymerase activity (gray) after the addition of dNTPs and exonuclease activity (black) after the addition of ptDNA, in a 10 min reaction at 70 °C (polymerase activity) or 55 °C (exonuclease activity). The error bars represent the standard error from at least three independent experiments. (C) Thermal melting of Dpo3 alone (gray dashed line) or bound (black solid line) to hairpin DNA monitored by circular dichroism at 222 nm (2 °C increments).

Conserved Mutations in the Polymerase Active Site Disrupt Activity. There is a conserved aspartic acid residue (D424) within the polymerase VI (Pol VI) domain and a single aspartic acid (D542) within the polymerase I (Pol I) domain of Dpo3 (Figure 3A). It has been previously shown that mutation of the conserved active site aspartates in homologous DNA polymerases abolishes nucleotide incorporation ability.[36−39] Interestingly, Dpo3 lacks the first aspartate in the highly conserved DTD motif in the Pol I domain (Figure 3A) known to be important for coordinating Mg^{2+} and contributing to translocation.[37] To determine if the polymerase active site of Dpo3

dx.doi.org/10.1021/bi201799a | *Biochemistry* 2012, 51, 1996−2007

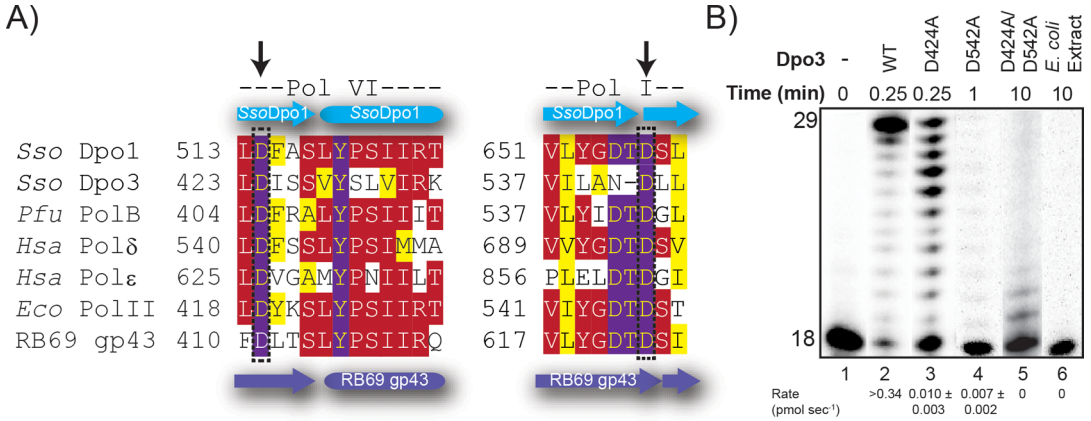

Figure 3. (A) Amino acid alignment of DNA polymerase domains VI and I using CLUSTAL W2 (http://www.ebi.ac.uk/Tools/clustalw2) for common members within the B-family of DNA replication polymerases. Slightly (yellow), mostly (red), and absolutely (purple) conserved residues are denoted. The secondary structure elements are derived from the crystal structure of Dpo1 (cyan) (PDB entry 1S5J) or RB69 gp43 (purple) (PDB entry 1CLQ). Species are identified with three-letter codes: *Sso*, *S. solfataricus*; *Pfu*, *Pyrococcus furiosus*; *Hsa*, *Homo sapiens*; *Eco*, *E. coli*. Arrows denote the residues in Dpo3 that were mutated and constitute the active site aspartates. (B) Effect of Dpo3 single (D424A or D542A) or double (D424A/D542A) mutants on the extension of template (T)G at 60 °C for the indicated times under optimal buffer conditions. The average rates in picomoles per second from multiple independent experiments are listed below the corresponding lanes of the gel.

is functionally conserved in the absence of a conserved Pol I domain, we constructed three mutants: two single mutants (D424A and D542A) and one double mutant (D424A/D542A). We then examined the polymerase activity of the mutants compared to that of WT Dpo3 at 60 °C (Figure 3B). The polymerase activity for the synthesis of full-length products for the D424A mutant was reduced more than 30-fold (0.010 ± 0.003 pmol/s) from the WT value (0.34 pmol/s), while that of the D542A mutant was reduced more than 50-fold (0.007 ± 0.002 pmol/s). The activity of the double mutant (D424A/D542A) was reduced to just above background levels and required much longer times for detection of any product.

Conserved Mutations in the Exonuclease Active Site Disrupt Activity. The exonuclease domain of polymerases can be organized into three motifs (Exo I, Exo II, and Exo III). Aspartates within each domain have been implicated in the proofreading function in different polymerases. Dpo3 has a conserved aspartate (D172) in the exonuclease I domain shown to be important for *E. coli* Pol II[40] and pol ε,[41] but mutation to alanine had no effect on exonuclease activity (data not shown). Examination of the exonuclease II motif (Exo II) showed no universally conserved aspartate or glutamate[42−44] for Dpo3, but it did contain four potential catalytic aspartates (Figure 4A). We individually mutated each aspartate (D226A, D228A, D234A, and D236A) in Exo II and examined their effect on the exonuclease activity levels on three DNA substrates (ssDNA, ptDNA, and dsDNA). As proof that D236 is involved in proofreading, the D236A mutant incorporates nucleotides fully to the end of the template unlike WT, which stops one base prior from the end (−1) in this time frame (Figure 4B). D236A had the lowest exonuclease activity and therefore produced the greatest perturbation (Figure 4C,D) of the four mutants. D234A/D236A produced no further reduction in exonuclease activity over the D236A single mutant (data not shown). The rate for formation of the exonuclease product for WT was 0.031 ± 0.001 pmol/s, while the rate for D236A was reduced approximately 7-fold to 0.0046 ± 0.0003 pmol/s, implicating this aspartate in the proofreading mechanism (Figure 4E).

DNA Binding Affinity of Dpo3 Monitored by Fluorescence Anisotropy. DNA binding of B-family polymerases is typically robust and shows a preference for ptDNA over ssDNA.[42] To determine if the relatively high concentrations of Dpo3 required for activity are a result of a weak binding affinity, we measured the DNA binding properties using fluorescence anisotropy. Fluorescence anisotropy measures the rotational diffusion rates of molecules, where a decrease in these rates using fluorescently labeled DNA occurs upon formation of a protein−DNA complex. The resulting increase in anisotropy (r) can be plotted to determine the binding coefficient (K_d). Both ssDNA and ptDNA were used as the substrate with a fluorescent dye, Cy3, located at the 5′-end of the template or single strand. Anisotropy values were measured as the Dpo3 concentration was increased. The K_d for the interaction between Dpo3 and ssDNA was 1.10 ± 0.08 μM, while the K_d for the interaction between ptDNA was tighter at 0.81 ± 0.06 μM (Figure 5).

Correct Nucleotide Specificity. We analyzed the pre-steady-state dNTP incorporation rate of the Dpo3 exonuclease mutant (D236A) for correctly paired nucleotides across from all four different template bases. These reactions could be performed accurately by hand at 37 °C because of a decreased rate of synthesis at lower temperatures. Previously, Suo and coworkers established that fidelity reactions with Dpo1 and Dpo4 performed at lower temperatures did not have values significantly different from those for reactions performed at higher temperatures.[22,45] Single-turnover reactions were performed in which the enzyme concentration (2 μM) was held well above the DNA concentration (9.6 nM) as required based on the affinities and activities measured above. The quantified products for different concentrations of dCTP incorporated onto template G were plotted as a function of the reaction times to obtain the apparent rate constants (k_{obs}) according to eq 3 (Figure 6A). These single-turnover rates were plotted as a function of the concentration of dCTP and fit to eq 4 to yield the second-order polymerization rate (k_p) (0.045 ± 0.007 s^{-1}) and dissociation constant for dCTP (K_d) (61 ± 25 μM) (Figure 6B and Table 1). The measure of substrate specificity (k_p/K_d) was calculated to be 7.4 × 10^{-3} μM^{-1} s^{-1}. If Dpo3 is able to bind nucleotides nonspecifically in the absence of DNA, high concentrations of enzyme could affect the K_d value measured if the concentration of enzyme was similar in magnitude. In our experiments, a large excess of enzyme was required to promote

dx.doi.org/10.1021/bi201799a | *Biochemistry* 2012, 51, 1996−2007

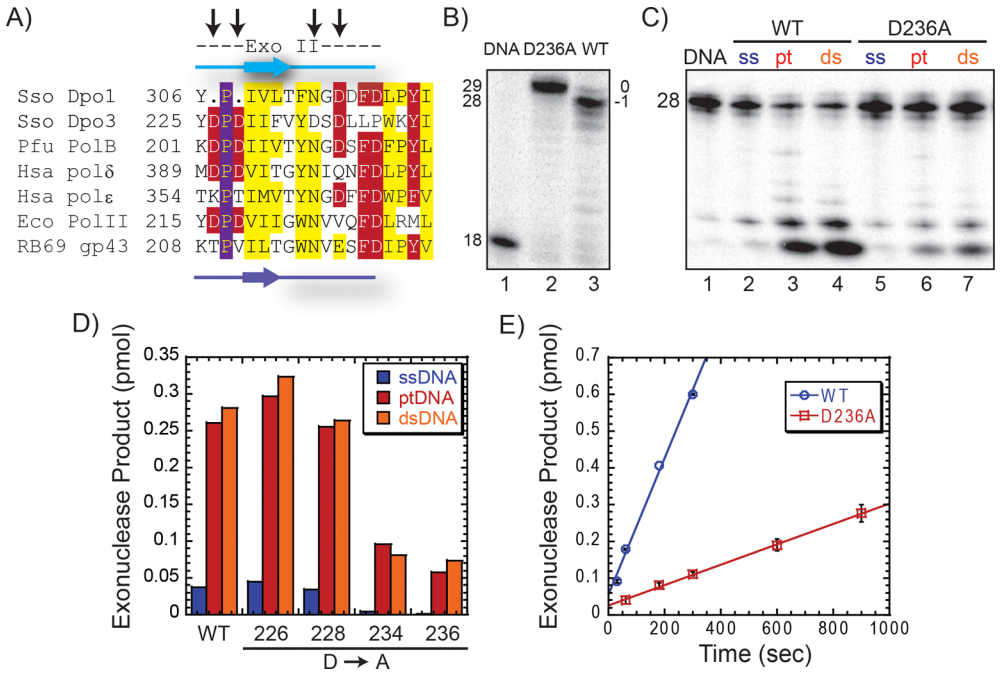

Figure 4. (A) Amino acid alignment of exonuclease domain II using CLUSTAL W2 (http://www.ebi.ac.uk/Tools/clustalw2) for common members within the B-family of DNA replication polymerases. Slightly (yellow), mostly (red), and absolutely (purple) conserved residues are denoted. The secondary structure elements are derived from the crystal structure of Dpo1 (cyan) (PDB entry 1S5J) or RB69 gp43 (purple) (PDB entry 1CLQ). Species are identified with three-letter codes: *Sso*, *S. solfataricus*; *Pfu*, *P. furiosus*; *Hsa*, *H. sapiens*; *Eco*, *E. coli*. Arrows denote the residues in Dpo3 that were mutated. (B) Polymerase reactions comparing formation of the full-length product from WT and D236A Dpo3 on template T at 70 °C for 3 min, showing major products (29 base, blunt, 0) or (28 base, recessed, −1) for D236A or WT Dpo3, respectively. (C) Exonuclease experiment with single-stranded (ssDNA), primer−template (ptDNA), and double-stranded (dsDNA) DNA for both WT and D236A Dpo3 at 55 °C for 10 min. (D) Quantification of exonuclease cleavage products for WT Dpo3 and each prospective exonuclease mutant (D226A, D228A, D234A, and D236A), on all three DNA conformations [ssDNA (blue), ptDNA (red), and dsDNA (orange)] at 55 °C for 10 min. (E) Quantification of the steady-state rate of exonuclease products produced from ptDNA by WT (0.031 ± 0.001 pmol/s) or D236A (0.0046 ± 0.0003 pmol/s) Dpo3 from at least two independent experiments. The error bars represent the standard error of the reaction.

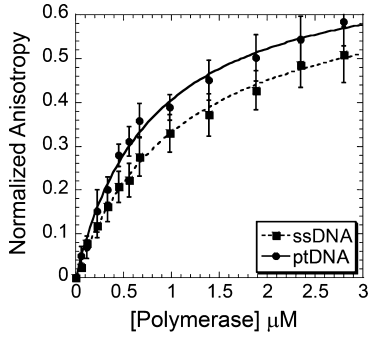

Figure 5. Change in fluorescence anisotropy upon binding of Dpo3 (D236A) to either Cy3-labeled ssDNA (Cy3DNA) (gray dashed line) or ptDNA (black solid line). Data points were fit to eq 4 to extract a K_d of binding for ssDNA (1.10 ± 0.08 μM) and ptDNA (0.81 ± 0.06 μM). The error bars represent the standard error from at least three independent experiments.

DNA binding, but this concentration is still at least 5−100 times lower than the experimental concentration of dCTP.

Single-turnover experiments for other correct nucleotide incorporations (dTTP on template A, dGTP on template C, and dATP on template T) were also performed similarly (Figure S3 of the Supporting Information). The kinetic parameters (k_p, K_d, and k_p/K_d) are listed in Table 1. Interesting observations from this analysis include the fact incorporation of dATP on template T was roughly 3-fold faster (0.12 ± 0.01 s^{-1}) than the reverse incorporation (dTTP on template A) (0.038 ± 0.002 s^{-1}). Also, the K_d for binding dATP was 3-fold tighter than for binding dCTP or dTTP on their respective correctly base paired templates.

Incorrect Nucleotide Specificity. Pre-steady-state incorporation rates for incorrect nucleotides opposite all four templates were also analyzed similarly as described above. As an example, single-nucleotide misincorporation of dTTP at various concentrations onto template T is shown in Figure 7A, yielding k_{obs}. These observed rates were plotted versus the dTTP concentration and fit to eq 4 to give k_p (0.0015 ± 0.0001 s^{-1}), K_d (0.39 ± 0.08 mM), and k_p/K_d (3.7 × 10^{-6} μM^{-1} s^{-1}) values (Figure 7B and Table 1). Misincorporation of dTTP on template T was roughly 100-fold slower and had a 20-fold weaker K_d than correct incorporation of dATP. This results in a misincorporation frequency for incorrect dNTPs of 5.4 × 10^{-4} (Table 1) or 1 error every 2000 bases with polymerase active site selection alone.

In some cases, inhibition was noted at high concentrations of incorrect nucleotides. Incorporation of dGTP on template T was inhibited at concentrations greater than 2 mM, and incorporation of dGTP on template G was inhibited at concentrations greater than 1 mM. Nucleotide selection seems to be the most discriminative for template C and template T provided by a concomitant decrease in both the polymerization rate and the affinity.

For the most part, incorrect nucleotide incorporations are 20−100 times slower than correct incorporations with K_d values 4−30 times weaker (Table 1). One exception seems to

dx.doi.org/10.1021/bi201799a | *Biochemistry* 2012, 51, 1996−2007

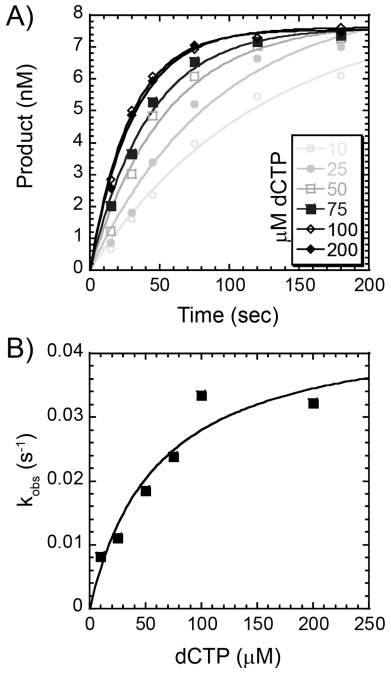

Figure 6. Concentration dependence of the pre-steady-state rate of correct nucleotide incorporation. (A) A preincubated solution containing 2 μM Dpo3 and template G (9.6 nM) was mixed with increasing concentrations of dCTP (from 10 to 200 μM) for the indicated time points. The data were fit to eq 3 to determine the single-exponential rate (k_{obs}). (B) k_{obs} values were plotted as a function of dCTP concentration and fit with eq 4 to yield k_p (0.045 ± 0.008 s^{-1}) and K_d (61 ± 26 μM).

be that the K_d values of dGTP and dCTP are identical on template G. The 40-fold slower rate of incorporation for dGTP on that template is the only factor that provides for the selectivity in this case, leading to a weaker fidelity value of 2.77×10^{-2}.

For template G, the preceding base (−1) in the template is cytosine, which allows for the possibility that the strong binding of dGTP on template G noted above is the result of a looping mechanism that base pairs the incoming nucleotide at position −1 in the template. To test this, we changed the base at position −1 in the template strand to T to create template (T)G. When single-nucleotide misincorporation assays were performed with dGTP on this template, there was a significant increase in the K_d to 0.69 ± 0.20 mM (Table 1). This resulted in a decrease in k_p/K_d (3.1×10^{-6} μM^{-1} s^{-1}) and misincorporation frequency (4.4×10^{-3}) more consistent with the rest of Table 1. Except for dGTP on template G, the error frequencies for Dpo3 range from 10^{-3} to 10^{-4} and are in line with those of other polymerases in this family.[46,47]

DISCUSSION

We have biochemically characterized both the DNA polymerization and exonuclease activities of the third B-family DNA polymerase in *S. solfataricus* and verified that it is an active enzyme. Although Dpo3 is characterized as a B-family DNA polymerase, the Pol I motif in the active site is not absolutely conserved, prompting speculation that it may be inactive.[48] Dpo3 was proposed to have evolved thorough a gene duplication event,[26] which eventually became the precursor for the human DNA polymerase ε implicated in leading strand DNA replication in eukaryotes.[7,19] To improve our understanding of the role of Dpo3 in chromosomal maintenance in archaea, we investigated the polymerase and exonuclease activities, fidelity, and thermostability of this polymerase.

Dpo3 is an accurate B-family DNA polymerase whose fidelity is increased further with the inclusion of an active exonuclease domain. Dpo3 has high thermostability that is increased slightly in the presence of DNA. Surprisingly, Dpo3 binds DNA weakly compared with other B-family polymerases,[22,23,42] and the exonuclease and polymerase activities are maximal at different

Table 1. Pre-Steady-State Kinetic Parameters of Dpo3

dNTP	k_p (s^{-1})[a]	K_d (mM)[a]	k_p/K_d (μM^{-1} s^{-1})	misincorporation frequency[b]
template A				
dATP	0.0010 ± 0.0002	0.23 ± 0.02	4.5×10^{-6}	6.7×10^{-3}
dCTP	0.0016 ± 0.0002	2.0 ± 0.6	7.9×10^{-7}	1.2×10^{-3}
dGTP	0.0017 ± 0.0004	1.7 ± 1.1	9.6×10^{-7}	1.5×10^{-3}
dTTP	0.038 ± 0.002	0.057 ± 0.008	6.6×10^{-4}	
template C				
dATP	0.00065 ± 0.00005	0.74 ± 0.20	8.9×10^{-7}	3.0×10^{-4}
dCTP[c]	–	–	–	–
dGTP	0.069 ± 0.005	0.024 ± 0.007	2.9×10^{-3}	
dTTP	0.0013 ± 0.0001	0.43 ± 0.16	3.1×10^{-6}	1.1×10^{-3}
template G				
dATP	0.0025 ± 0.0005	1.9 ± 0.9	1.3×10^{-6}	1.9×10^{-3}
dCTP	0.045 ± 0.008	0.061 ± 0.025	7.4×10^{-4}	
dGTP[d]	0.0011 ± 0.0001	0.056 ± 0.017	2.0×10^{-5}	2.8×10^{-2}
dTTP	0.0016 ± 0.0001	0.30 ± 0.08	5.3×10^{-6}	7.6×10^{-3}
template (T)G				
dGTP	0.0021 ± 0.0002	0.69 ± 0.20	3.1×10^{-6}	4.4×10^{-3}
template T				
dATP	0.12 ± 0.01	0.018 ± 0.006	6.8×10^{-3}	
dCTP	0.0009 ± 0.0001	0.79 ± 0.34	1.1×10^{-6}	1.6×10^{-4}
dGTP[e]	0.0025 ± 0.0001	0.41 ± 0.03	6.0×10^{-6}	8.7×10^{-4}
dTTP	0.0015 ± 0.0001	0.39 ± 0.08	3.7×10^{-6}	5.4×10^{-4}

[a]Calculated from the fit to eq 4 of the second-order plot. [b]Calculated as $(k_p/K_d)_{incorrect}/(k_p/K_d)_{correct}$. [c]Was not incorporated appreciably above background and could not be quantified. [d]Inhibition at >1 mM dGTP. [e]Inhibition at >2 mM dGTP.

dx.doi.org/10.1021/bi201799a | *Biochemistry* 2012, 51, 1996−2007

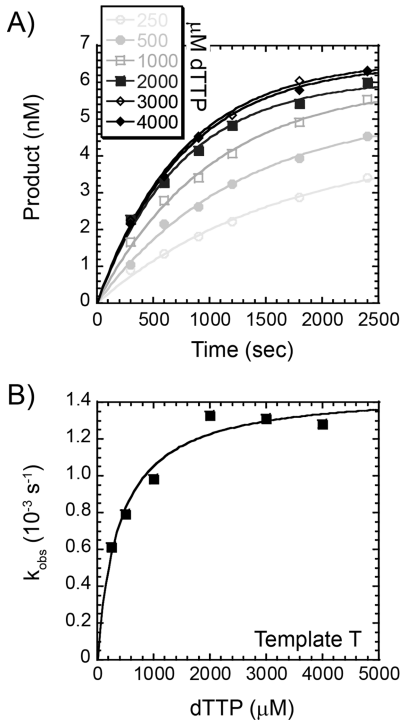

Figure 7. Concentration dependence of the pre-steady-state rate of incorrect nucleotide incorporation. (A) A preincubated solution containing 2 μM Dpo3 and template T (9.6 nM) was mixed with increasing concentrations of dTTP (from 250 μM to 4 mM) for the indicated time points. The data were fit to eq 3 to determine the single-exponential rate (k_{obs}). (B) k_{obs} values were plotted as a function of dTTP concentration and fit with eq 4 to yield k_p (0.0015 ± 0.0001 s^{-1}) and K_d (0.39 ± 0.08 mM).

temperatures. While our manuscript was being prepared, a recent report also characterized the in vitro activity of Dpo3,[28] and although there are some similarities such as weak DNA binding, we have measured significant differences in the kinetic and thermodynamic parameters as well as verified and compared the importance of the catalytic residues in the polymerase and exonuclease active sites. In spite of the nonconserved active site motifs, Dpo3 has been confirmed to be a B-family DNA polymerase with enzymatic activities that allow participation in coupled DNA replication or repair activities in archaea. The roles and activities of multiple DNA polymerases in this organism provide a model for understanding and characterizing DNA polymerase specificities in higher organisms.

Nonconserved Polymerase Motifs Reduce DNA Binding and Enzymatic Activity. Although Dpo3 is considered to be a B-family DNA polymerase, the most conserved Pol I domain contained in all DNA polymerases is mutated. This conserved YGDTD sequence is used to coordinate Mg^{2+} where the tyrosine and both aspartates are thought to be essential for polymerase activity.[37,38,49] In Dpo3, the homologous sequence is LAN-D, where rather than a pair of aspartic acids residues coordinating Mg^{2+} and contributing to translocation, a single aspartic acid residue is important for catalytic activity. Crystal structures of RB69 gp43[34] and yeast pol δ[50] highlight the importance of the second aspartate (Pol I) in metal coordination and catalysis, which is consistent with a similar role for D542 in Dpo3.

Conversely, the first aspartate in the Pol I motif is generally orientated away and toward the minor groove at the site of insertion.[51,52] Although this first aspartate is conserved, the actual role of this residue is elusive. Mutation of the first aspartate (Pol I) in Phi29 DNA polymerase disrupted the translocation step between catalysis steps and resulted in a lower processivity, possibly representing a looser grip on DNA.[53] Interestingly, high concentrations of Dpo3 (>750 nM) were required for stable binding and efficient DNA extension as also noted previously[28] and could be the consequence of the missing first aspartate. Mutation of the homologous first aspartate in human polymerase α required Mn^{2+} for restoration of the wild-type activity.[38] Our metal-dependent studies of Dpo3 may actually be similar in that at metal concentrations of <1 mM, Mn^{2+} provides the optimal activity. At higher concentrations, Mn^{2+} is inhibitory and Mg^{2+} provides for optimal activity similar to the D1002N mutant of human pol α.[38]

The other catalytic aspartate contained in the Pol VI motif and known to be involved in Mg^{2+} coordination is conserved in Dpo3 (D424), but residues adjacent to this residue have also been shown to affect catalysis. Previous work by Kennedy et al. implicated a conserved ALY motif within the Pol VI domain of the *P. furiosus* B-family polymerase in a stacking interaction with the ribose of the incoming nucleotide.[54] A408S and L409V

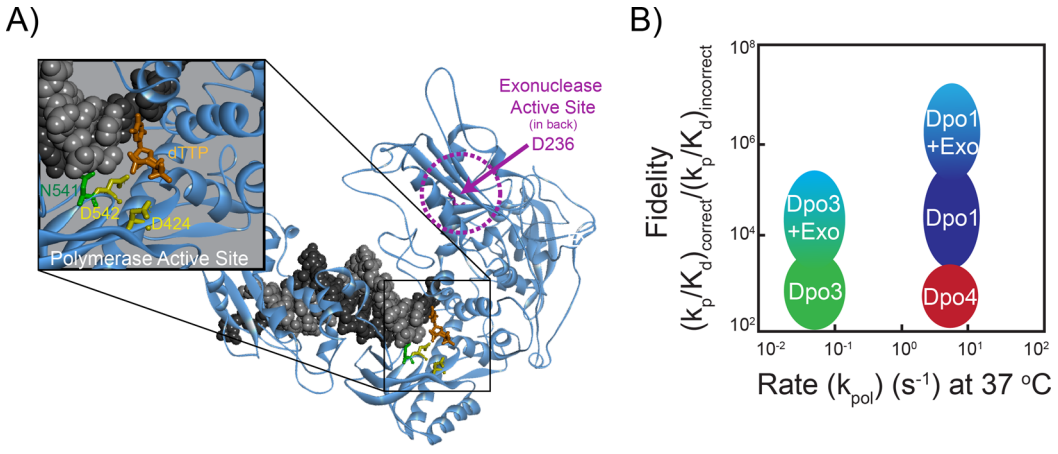

Figure 8. (A) Homology model of the ternary complex of Dpo3 bound to DNA (black and gray) with incoming dTTP (orange) highlighting the aspartates in the polymerase (D424 and D542, yellow) and exonuclease (D236, pink) active sites. N541 (green) is also shown oriented toward the minor groove of the dsDNA template. (B) Graphical representation of the fidelity $[(k_p/K_d)_{correct}/(k_p/K_d)_{incorrect}]$ as a function of the rate (k_{pol}) comparing Dpo1, Dpo3, and Dpo4.

dx.doi.org/10.1021/bi201799a | *Biochemistry* 2012, 51, 1996–2007

mutations in *Pfu* Pol both result in a decrease in the catalytic efficiency (k_{cat}/K_m). It seems that increased side chain volume interacting at the back of the incoming nucleotide negatively affects catalysis and fidelity. The homologous wild-type sequence in Dpo3 is 427-SVY and may also contribute to Dpo3's slower incorporation rates and reduced fidelity.

To highlight the two active site aspartates primarily responsible for metal binding and catalysis, we created a ternary homology model of Dpo3 bound to DNA with an incoming dTTP (Figure 8A). In this model, it is clear that D424 and D542 are oriented properly for binding metals in the active site required for catalysis and incoming dNTP stabilization. Interestingly, N541 seems to adopt a conformational position similar to that of the first aspartate in the Pol I motif of other polymerases. The absence of a negative charge at this position in Dpo3 would disrupt native interactions with Mg^{2+} and the DNA template, possibly explaining the reduced affinity of binding.

Dpo3 Has Moderate Polymerase Activity. We have shown through detailed kinetic analysis that the catalytic activity of Dpo3 is moderate, although the rate of nucleotide incorporation is significantly faster than those previously published.[28] During the purification of Dpo3, it became clear that inclusion of a gel-filtration column for size selection and cleanup was required for maximal activity. A comparison of the reaction conditions used in our study with those from the previous report[28] noted no significant differences in extension rates using our purified protein. Polymerization reactions for Dpo3 at 37 or 50 °C converted more than 50−70% of the substrate to full-length product in 10 min (Figure 2A) compared with little full-length product formed at these temperatures in a 30 min reaction described previously.[28] The kinetic rate constants are difficult to compare between the studies, because we used pre-steady-state analysis monitoring the fastest rate of single-nucleotide incorporation for Dpo3, while the previous study used steady-state analysis. Pre-steady-state analysis has been shown to be more accurate for measuring the kinetic and thermodynamic basis for the fidelity of nucleotide incorporation.[55] Moreover, we have verified that Dpo3 has an active exonuclease proofreading domain that would make steady-state analysis of polymerase fidelity with the wild-type enzyme difficult.

The fidelities of nucleotide incorporation for the Dpo3 polymerase active site alone are generally 10^2−10^3. One exception where the fidelity is lower occurs when the incoming base is incorporated on the basis of complementarity to the preceding −1 template base (dGTP on template G). In this case, incorporation would require destabilization of the terminal base pair and looping out of the last base in the primer strand. Incorporation would then proceed opposite the −1 base in the template. An analogous looping out mechanism has been noted previously for Dpo4,[56,57] although the looped-out base occurs in the template strand instead, in favor of nucleotide incorporation opposite position +1. We can rule out a similar mechanism for Dpo3 as incorporation of dATP in template G (where the +1 base is T) has the weakest K_d value of the group.

In general, the pre-steady-state kinetics of Dpo3 are reduced compared with those of the other two well-characterized DNA polymerases (Dpo1 and Dpo4) in *Sso* (Table 2). We compared the nucleotide binding, kinetic incorporation rate, and fidelity differences of Dpo3 with those of Dpo1 and Dpo4. Dpo3 possesses nucleotide selectivity (K_d difference) values more similar to that of the Y-family DNA polymerase, Dpo4. The ratio of the maximal rate of incorporation (k_p) for correct versus incorrect nucleotides for Dpo3 is more similar to the selectivity provided by Dpo1, although the absolute rate of catalysis is roughly 100-fold slower. Therefore, the fidelity of Dpo3 is primarily driven by a reduced rate of incorporation for incorrect nucleotides rather than selectivity in nucleotide binding. The fidelity values for Dpo3 are comparable to those for Dpo4 but lower than those for Dpo1 (Table 2). The exonuclease domain contained within Dpo3 will increase the fidelity value further, approaching that required for accurate DNA synthesis making this polymerase more accurate than Dpo4 (Figure 8B).

Table 2. *S. solfataricus* DNA Polymerase Comparison

polymerase	fidelity $(k_p/K_d)_{correct}/(k_p/K_d)_{incorrect}$	K_d difference $(K_d)_{incorrect}/(K_d)_{correct}$	k_p difference $(k_p)_{correct}/(k_p)_{incorrect}$
Dpo3[a]	1.5×10^2 to 6.3×10^3	4−45	17−140
Dpo1[b]	1.6×10^3 to 2.9×10^5	110−920	4−580
Dpo4[c]	3.1×10^2 to 6.7×10^3	1−18	99−1600

[a]At 37 °C (from this work). [b]At 37 °C;[23] data do not include the fidelity contribution from the 3′−5′ exonuclease activity. [c]At 37 °C.[22]

Variable Thermostabilities of the Polymerase and Exonuclease Domains. Interestingly, the temperatures at which the polymerase and exonuclease activities are maximal are different. The maximal exonuclease activity occurs at 55 °C, which is below the physiological temperature, while the maximal polymerase activity occurs above 65 °C. The thermostability of the entire Dpo3 structure is high with a T_m of >94 °C, which is increased slightly in the presence of DNA. This is in direct contrast to a previous report that showed that preincubation for 20 min at 60 °C completely abolished activity.[28] Conversely, we can show that preincubation at 70 °C for 55 min only minimally reduces polymerase activity, and the exonuclease domain retains more than half of the original activity. Thermostabilites for Dpo1 and Dpo4 have been measured previously[58,59] and are similar to that found for Dpo3.

Looking closely at the CD spectra, we have noticed a reproducible but slight deviation around 63 °C, suggesting that a local reversible unfolding event may be possible. This spectral change is not observed when DNA is included in the experiment, suggesting that a more stable protein complex exists in the presence of DNA, possibly representing the closed conformation. On the basis of the decrease in promiscuous exonuclease activity above 55 °C and the change in the CD spectra at 63 °C, we conclude that the exonuclease domain is stabilized in a proofreading conformation in the presence of DNA at high temperatures.

When dNTPs are included, the role of the exonuclease activity is to increase the fidelity by monitoring correct base incorporations. Clearly, there is a cycle between nucleotide incorporation and exonuclease proofreading that occurs with the wild-type enzyme similar to that in other B-family DNA polymerases. The exonuclease activity is controlled by the kinetics of the forward rate constant for nucleotide incorporation. When dNTPs are absent or present at low levels, the kinetic rate of incorporation is low and causes the slightly slower exonuclease rate to proceed instead. For Dpo3, the exonuclease activity is somewhat temperature-dependent. The change in the CD spectrum coupled with the slower kinetics at higher

temperatures suggests that the DNA binding specificity (ssDNA or ptDNA) may be modulated by temperature. This may also help explain the lower exonuclease activity on ssDNA versus ptDNA at higher temperatures in spite of somewhat similar affinities. Even so, the recognition or proofreading of misincorporated bases opposite damaged templates (hypoxanthine, 8-oxoG, and cyclobutane dimers) may be less restrictive in some cases depending on the geometry as Dpo3 has been shown recently to be able to bypass these lesions.[28]

Role of Multiple B-Family DNA Polymerases in Archaea. The DNA replication system from *Sulfolobus* is now an even more enticing model system with the discovery that there are multiple active B-family DNA polymerases along with a single Y-family lesion bypass polymerase. This is similar to the cases in other organisms that have multiple DNA replication polymerases at the replication fork.[7,60] The measured in vitro activity of Dpo3 is absolutely slower than that of the proposed DNA replication polymerase, Dpo1 (Figure 8B). Therefore, it seems that Dpo1 will provide the major replicative activity during replication. Of course, we cannot rule out an increase in activity for Dpo3 with additional accessory factors *in vivo*. The included active exonuclease proofreading domain of Dpo3 would suggest that it has a role in faithful DNA replication and not necessarily repair or lesion bypass. Of course, genetic knockouts of this polymerase could provide some further information about the proposed role in genomic maintenance.

DNA binding and recognition of the DNA template will be difficult for Dpo3 because of its weaker affinity. We have shown previously that Dpo1 can form a trimeric complex in a similar concentration range.[42] It was noted recently that the protein expression levels of Dpo3 are similar to those of Dpo1 and much greater than those of Dpo4,[28] suggesting that the cellular concentrations and thermodynamics may favor formation of a Dpo3−DNA complex. Therefore, the local concentrations of polymerases around the replication fork will strongly influence associations.

On the basis of the enzymatic properties described here, Dpo3 could be involved in initiating DNA replication, in extension of Okazaki fragments on the lagging strand,[61] or in a more directed role of synthesis across specific lesions.[28] The initiation of DNA replication after RNA priming is performed by DNA polymerase α in humans. There is no direct homologue in archaea, and the polymerase responsible for extending the RNA primer to initiate DNA replication has not been identified.[62] The measured in vitro synthesis rate of Dpo3 extrapolated at 75 °C is roughly 150 s^{-1}, based on the rate increase measured with temperature for Dpo1.[22] This is slightly faster than that required (92 s^{-1}) for bidirectional synthesis of the leading strand at three origins[63] on the *Sso* genome (2.99×10^6 bases)[64] over a 90 min S-phase.[65] It is equally possible that synthesis of the short 100−150-base Okazaki fragments[66] could be performed by Dpo3 in parallel to provide the necessary speed for genomic replication. Probably just as likely though, Dpo3 could be confined to a specialized role in DNA repair, although with the identification of an active exonuclease domain, the specific lesions that are processed remain to be determined. Identification of protein partners interacting with Dpo3 may be able to better reveal a potential role for this polymerase *in vivo*. Clearly, there are multiple kinetic and thermodynamic association events that occur with DNA in an organism with multiple DNA polymerases. The regulation of each DNA polymerase's individual activity will be dynamically controlled by cellular concentrations and interactions with other accessory proteins that direct binding along with their individual kinetics to maintain the genome.

■ ASSOCIATED CONTENT

Supporting Information

DNA substrates (Table S1), DNA primers (Table S2), buffer and metal optimization (Figure S1), example gels of the time course of incorporation for polymerase active site mutants (Figure S2), and additional pre-steady-state correct incorporation second-order plots (Figure S3). This material is available free of charge via the Internet at http://pubs.acs.org.

■ AUTHOR INFORMATION

Corresponding Author

*Address: 219 Parkman Ave., 801 Chevron, Pittsburgh, PA 15260. Telephone: (412) 624-1204. Fax: (412) 624-8611. E-mail: mtraksel@pitt.edu.

Funding

Funding was provided by startup funds from the University of Pittsburgh, Department of Chemistry (M.A.T.), and a Research Scholar Grant (RSG-11-049-01-DMC) to M.A.T. from the American Cancer Society.

Notes

The authors declare no competing financial interest.

■ ACKNOWLEDGMENTS

We thank Hsiang-Kai Lin for performing the circular dichroism experiments and Brian Graham for critical reading of the manuscript.

■ ABBREVIATIONS

Sso, *S. solfataricus*; Dpo1, *Sso* DNA polymerase I; Dpo2, *Sso* DNA polymerase II; Dpo3, *Sso* DNA polymerase III; CD, circular dichroism; ssDNA, single-stranded DNA; ptDNA, primer−template DNA; dsDNA, double-stranded DNA; T_m, thermal melting temperature; K_d, dissociation constant; k_p, pre-steady-state rate constant; k_{obs}, observed rate constant; K_d', apparent dissociation constant; WT, wild-type.

■ REFERENCES

(1) Filee, J., Forterre, P., Sen-Lin, T., and Laurent, J. (2002) Evolution of DNA polymerase families: Evidences for multiple gene exchange between cellular and viral proteins. *J. Mol. Evol. 54*, 763−773.

(2) Burgers, P. M., Koonin, E. V., Bruford, E., Blanco, L., Burtis, K. C., Christman, M. F., Copeland, W. C., Friedberg, E. C., Hanaoka, F., Hinkle, D. C., Lawrence, C. W., Nakanishi, M., Ohmori, H., Prakash, L., Prakash, S., Reynaud, C. A., Sugino, A., Todo, T., Wang, Z., Weill, J. C., and Woodgate, R. (2001) Eukaryotic DNA polymerases: Proposal for a revised nomenclature. *J. Biol. Chem. 276*, 43487−43490.

(3) Hubscher, U., Maga, G., and Spadari, S. (2002) Eukaryotic DNA polymerases. *Annu. Rev. Biochem. 71*, 133−163.

(4) Bebenek, K., and Kunkel, T. A. (2004) Functions of DNA polymerases. *Adv. Protein Chem. 69*, 137−165.

(5) Kunkel, T. A., and Bebenek, K. (2000) DNA replication fidelity. *Annu. Rev. Biochem. 69*, 497−529.

(6) Jeruzalmi, D., O'Donnell, M., and Kuriyan, J. (2002) Clamp loaders and sliding clamps. *Curr. Opin. Struct. Biol. 12*, 217−224.

(7) Nick McElhinny, S. A., Gordenin, D. A., Stith, C. M., Burgers, P. M., and Kunkel, T. A. (2008) Division of labor at the eukaryotic replication fork. *Mol. Cell 30*, 137−144.

(8) Beckman, J., Kincaid, K., Hocek, M., Spratt, T., Engels, J., Cosstick, R., and Kuchta, R. D. (2007) Human DNA polymerase α uses a combination of positive and negative selectivity to polymerize purine dNTPs with high fidelity. *Biochemistry 46*, 448−460.

(9) Burgers, P. M. (2009) Polymerase dynamics at the eukaryotic DNA replication fork. *J. Biol. Chem. 284*, 4041−4045.
(10) Kuchta, R. D., and Stengel, G. (2010) Mechanism and evolution of DNA primases. *Biochim. Biophys. Acta 1804*, 1180−1189.
(11) Stillman, B. (2008) DNA polymerases at the replication fork in eukaryotes. *Mol. Cell 30*, 259−260.
(12) Grabowski, B., and Kelman, Z. (2003) Archeal DNA replication: Eukaryal proteins in a bacterial context. *Annu. Rev. Microbiol. 57*, 487−516.
(13) Barry, E. R., and Bell, S. D. (2006) DNA replication in the archaea. *Microbiol. Mol. Biol. Rev. 70*, 876−887.
(14) Majernik, A. I., Jenkinson, E. R., and Chong, J. P. (2004) DNA replication in thermophiles. *Biochem. Soc. Trans. 32*, 236−239.
(15) Leipe, D. D., Aravind, L., and Koonin, E. V. (1999) Did DNA replication evolve twice independently? *Nucleic Acids Res. 27*, 3389−3401.
(16) Cann, I. K. O., Komori, K., Toh, H., Kanai, S., and Ishino, Y. (1998) A heterodimeric DNA polymerase: Evidence that members of Euryarchaeota possess a distinct DNA polymerase. *Proc. Natl. Acad. Sci. U.S.A. 95*, 14250−14255.
(17) Kulaeva, O. I., Koonin, E. V., McDonald, J. P., Randall, S. K., Rabinovich, N., Connaughton, J. F., Levine, A. S., and Woodgate, R. (1996) Identification of a DinB/UmuC homolog in the archeon *Sulfolobus solfataricus*. *Mutat. Res. 357*, 245−253.
(18) Gruz, P., Shimizu, M., Pisani, F. M., De Felice, M., Kanke, Y., and Nohmi, T. (2003) Processing of DNA lesions by archaeal DNA polymerases from *Sulfolobus solfataricus*. *Nucleic Acids Res. 31*, 4024−4030.
(19) Tahirov, T. H., Makarova, K. S., Rogozin, I. B., Pavlov, Y. I., and Koonin, E. V. (2009) Evolution of DNA polymerases: An inactivated polymerase-exonuclease module in Pol ε and a chimeric origin of eukaryotic polymerases from two classes of archaeal ancestors. *Biol. Direct 4*, 11.
(20) Brown, J. A., and Suo, Z. (2009) Elucidating the kinetic mechanism of DNA polymerization catalyzed by *Sulfolobus solfataricus* P2 DNA polymerase B1. *Biochemistry 48*, 7502−7511.
(21) Fiala, K. A., and Suo, Z. (2004) Mechanism of DNA polymerization catalyzed by *Sulfolobus solfataricus* P2 DNA polymerase IV. *Biochemistry 43*, 2116−2125.
(22) Zhang, L., Brown, J. A., Newmister, S. A., and Suo, Z. (2009) Polymerization fidelity of a replicative DNA polymerase from the hyperthermophilic archaeon *Sulfolobus solfataricus* P2. *Biochemistry 48*, 7492−7501.
(23) Fiala, K. A., and Suo, Z. (2004) Pre-steady-state kinetic studies of the fidelity of *Sulfolobus solfataricus* P2 DNA polymerase IV. *Biochemistry 43*, 2106−2115.
(24) Ling, H., Boudsocq, F., Woodgate, R., and Yang, W. (2001) Crystal structure of a Y-family DNA polymerase in action: A mechanism for error-prone and lesion-bypass replication. *Cell 107*, 91−102.
(25) Savino, C., Federici, L., Johnson, K. A., Vallone, B., Nastopoulos, V., Rossi, M., Pisani, F. M., and Tsernoglou, D. (2004) Insights into DNA replication: The crystal structure of DNA polymerase B1 from the archaeon *Sulfolobus solfataricus*. *Structure 12*, 2001−2008.
(26) Edgell, D. R., Klenk, H. P., and Doolittle, W. F. (1997) Gene duplications in evolution of archaeal family B DNA polymerases. *J. Bacteriol. 179*, 2632−2640.
(27) Prangishvili, D., and Klenk, H. P. (1993) Nucleotide sequence of the gene for a 74 kDa DNA polymerase from the archaeon *Sulfolobus solfataricus*. *Nucleic Acids Res. 21*, 2768.
(28) Choi, J. Y., Eoff, R. L., Pence, M. G., Wang, J., Martin, M. V., Kim, E. J., Folkmann, L. M., and Guengerich, F. P. (2011) Roles of the four DNA polymerases of the crenarchaeon *Sulfolobus solfataricus* and accessory proteins in DNA replication. *J. Biol. Chem. 286*, 31180−31193.
(29) Sambrook, J., and Russell, D. W. (2001) *Molecular Cloning: A Laboratory Manual*, Vol. *1*−*3*, Cold Spring Harbor Laboratory Press, Plainview, NY.
(30) Studier, F. W. (2005) Protein production by auto-induction in high density shaking cultures. *Protein Expression Purif. 41*, 207−234.
(31) Gill, S. C., and von Hippel, P. H. (1989) Calculation of protein extinction coefficients from amino acid sequence data. *Anal. Biochem. 182*, 319−326.
(32) Marky, L. A., and Breslauer, K. J. (1987) Calculating thermodynamic data for transitions of any molecularity from equilibrium melting curves. *Biopolymers 26*, 1601−1620.
(33) Arnold, K., Bordoli, L., Kopp, J., and Schwede, T. (2006) The SWISS-MODEL workspace: A web-based environment for protein structure homology modelling. *Bioinformatics 22*, 195−201.
(34) Franklin, M. C., Wang, J., and Steitz, T. A. (2001) Structure of the replicating complex of a pol α family DNA polymerase. *Cell 105*, 657−667.
(35) Hillebrand, G. G., and Beattie, K. (1984) Template-dependent variation in the relative fidelity of DNA polymerase I of *Escherichia coli* in the presence of Mg^{2+} versus Mn^{2+}. *Nucleic Acids Res. 12*, 3173−3183.
(36) Polesky, A. H., Steitz, T. A., Grindley, N. D., and Joyce, C. M. (1990) Identification of residues critical for the polymerase activity of the Klenow fragment of DNA polymerase I from *Escherichia coli*. *J. Biol. Chem. 265*, 14579−14591.
(37) Bernad, A., Blanco, L., and Salas, M. (1990) Site-directed mutagenesis of the YCDTDS amino acid motif of the phi29 DNA polymerase. *Gene 94*, 45−51.
(38) Copeland, W. C., and Wang, T. S. (1993) Mutational analysis of the human DNA polymerase α. The most conserved region in α-like DNA polymerases is involved in metal-specific catalysis. *J. Biol. Chem. 268*, 11028−11040.
(39) Dua, R., Levy, D. L., and Campbell, J. L. (1999) Analysis of the essential functions of the C-terminal protein/protein interaction domain of *Saccharomyces cerevisiae* pol ε and its unexpected ability to support growth in the absence of the DNA polymerase domain. *J. Biol. Chem. 274*, 22283−22288.
(40) Lowe, L. G., and Guengerich, F. P. (1996) Steady-state and pre-steady-state kinetic analysis of dNTP insertion opposite 8-oxo-7,8-dihydroguanine by *Escherichia coli* polymerases I exo- and II exo. *Biochemistry 35*, 9840−9849.
(41) Korona, D. A., Lecompte, K. G., and Pursell, Z. F. (2011) The high fidelity and unique error signature of human DNA polymerase ε. *Nucleic Acids Res. 39*, 1763−1773.
(42) Mikheikin, A. L., Lin, H. K., Mehta, P., Jen-Jacobson, L., and Trakselis, M. A. (2009) A trimeric DNA polymerase complex increases the native replication processivity. *Nucleic Acids Res. 37*, 7194−7205.
(43) Bebenek, A., Dressman, H. K., Carver, G. T., Ng, S., Petrov, V., Yang, G., Konigsberg, W. H., Karam, J. D., and Drake, J. W. (2001) Interacting fidelity defects in the replicative DNA polymerase of bacteriophage RB69. *J. Biol. Chem. 276*, 10387−10397.
(44) Fazlieva, R., Spittle, C. S., Morrissey, D., Hayashi, H., Yan, H., and Matsumoto, Y. (2009) Proofreading exonuclease activity of human DNA polymerase δ and its effects on lesion-bypass DNA synthesis. *Nucleic Acids Res. 37*, 2854−2866.
(45) Fiala, K. A., Sherrer, S. M., Brown, J. A., and Suo, Z. (2008) Mechanistic consequences of temperature on DNA polymerization catalyzed by a Y-family DNA polymerase. *Nucleic Acids Res. 36*, 1990−2001.
(46) Dieckman, L. M., Johnson, R. E., Prakash, S., and Washington, M. T. (2010) Pre-steady state kinetic studies of the fidelity of nucleotide incorporation by yeast DNA polymerase δ. *Biochemistry 49*, 7344−7350.
(47) Zhong, X., Pedersen, L. C., and Kunkel, T. A. (2008) Characterization of a replicative DNA polymerase mutant with reduced fidelity and increased translesion synthesis capacity. *Nucleic Acids Res. 36*, 3892−3904.
(48) Rogozin, I. B., Makarova, K. S., Pavlov, Y. I., and Koonin, E. V. (2008) A highly conserved family of inactivated archaeal B family DNA polymerases. *Biol. Direct 3*, 32.
(49) Blasco, M. A., Bernad, A., Blanco, L., and Salas, M. (1991) Characterization and mapping of the pyrophosphorolytic activity of the

phage phi29 DNA polymerase. Involvement of amino acid motifs highly conserved in α-like DNA polymerases. *J. Biol. Chem. 266*, 7904−7909.
(50) Swan, M. K., Johnson, R. E., Prakash, L., Prakash, S., and Aggarwal, A. K. (2009) Structural basis of high-fidelity DNA synthesis by yeast DNA polymerase δ. *Nat. Struct. Mol. Biol. 16*, 979−986.
(51) Zahn, K. E., Tchesnokov, E. P., Gotte, M., and Doublie, S. (2011) Phosphonoformic acid inhibits viral replication by trapping the closed form of the DNA polymerase. *J. Biol. Chem. 286*, 25246−25255.
(52) Xia, S., Wang, M., Blaha, G., Konigsberg, W. H., and Wang, J. (2011) Structural insights into complete metal ion coordination from ternary complexes of B family RB69 DNA polymerase. *Biochemistry 50*, 9114−9124.
(53) Saturno, J., Lazaro, J. M., Blanco, L., and Salas, M. (1998) Role of the first aspartate residue of the "YxDTDS" motif of phi29 DNA polymerase as a metal ligand during both TP-primed and DNA-primed DNA synthesis. *J. Mol. Biol. 283*, 633−642.
(54) Kennedy, E. M., Hergott, C., Dewhurst, S., and Kim, B. (2009) The mechanistic architecture of thermostable *Pyrococcus furiosus* family B DNA polymerase motif A and its interaction with the dNTP substrate. *Biochemistry 48*, 11161−11168.
(55) Johnson, K. A. (1992) Transient-State Kinetic Analysis of Enzyme Reaction Pathways. In *The Enzymes* (David, S. S., Ed.) pp 1−61, Academic Press, San Diego.
(56) Fiala, K. A., and Suo, Z. (2007) Sloppy bypass of an abasic lesion catalyzed by a Y-family DNA polymerase. *J. Biol. Chem. 282*, 8199−8206.
(57) Fiala, K. A., Hypes, C. D., and Suo, Z. (2007) Mechanism of abasic lesion bypass catalyzed by a Y-family DNA polymerase. *J. Biol. Chem. 282*, 8188−8198.
(58) Pisani, F. M., De Felice, M., and Rossi, M. (1998) Amino acid residues involved in determining the processivity of the 3′-5′ exonuclease activity in a family B DNA polymerase from the thermoacidophilic archaeon *Sulfolobus solfataricus*. *Biochemistry 37*, 15005−15012.
(59) Boudsocq, F., Iwai, S., Hanaoka, F., and Woodgate, R. (2001) *Sulfolobus solfataricus* P2 DNA polymerase IV (Dpo4): An archaeal DinB-like DNA polymerase with lesion-bypass properties akin to eukaryotic pol η. *Nucleic Acids Res. 29*, 4607−4616.
(60) McInerney, P., Johnson, A., Katz, F., and O'Donnell, M. (2007) Characterization of a triple DNA polymerase replisome. *Mol. Cell 27*, 527−538.
(61) Duggin, I. G., and Bell, S. D. (2006) The chromosome replication machinery of the archaeon *Sulfolobus solfataricus*. *J. Biol. Chem. 281*, 15029−15032.
(62) Zuo, Z., Rodgers, C. J., Mikheikin, A. L., and Trakselis, M. A. (2010) Characterization of a functional DnaG-type primase in archaea: Implications for a dual-primase system. *J. Mol. Biol. 397*, 664−676.
(63) Robinson, N. P., and Bell, S. D. (2005) Origins of DNA replication in the three domains of life. *FEBS J. 272*, 3757−3766.
(64) She, Q., Singh, R. K., Confalonieri, F., Zivanovic, Y., Allard, G., Awayez, M. J., Chan-Weiher, C. C., Clausen, I. G., Curtis, B. A., De, M. A., Erauso, G., Fletcher, C., Gordon, P. M., Heikamp-de, J. I., Jeffries, A. C., Kozera, C. J., Medina, N., Peng, X., Thi-Ngoc, H. P., Redder, P., Schenk, M. E., Theriault, C., Tolstrup, N., Charlebois, R. L., Doolittle, W. F., Duguet, M., Gaasterland, T., Garrett, R. A., Ragan, M. A., Sensen, C. W., and Van der, O. J. (2001) The complete genome of the crenarchaeon *Sulfolobus solfataricus* P2. *Proc. Natl. Acad. Sci. U.S.A. 98*, 7835−7840.
(65) Duggin, I. G., McCallum, S. A., and Bell, S. D. (2008) Chromosome replication dynamics in the archaeon *Sulfolobus acidocaldarius*. *Proc. Natl. Acad. Sci. U.S.A. 105*, 16737−16742.
(66) Matsunaga, F., Norais, C., Forterre, P., and Myllykallio, H. (2003) Identification of short 'eukaryotic' Okazaki fragments synthesized from a prokaryotic replication origin. *EMBO Rep. 4*, 154−158.